# Supplementary Information

# Uniform Yolk-Shell $Sn_4P_3$@C Nanospheres as High-Capacity and Cycle-Stable Anode Materials for Sodium-Ion Batteries

Jun Liu,[b,c] Peter Kopold,[b] Chao Wu,[b] Peter A. van Aken,[b] Joachim Maier[b] and Yan Yu[a,b]*

[a]Key Laboratory of Materials for Energy Conversion, Chinese Academy of Sciences, Department of Materials Science and Enginering, University of Science and Technology of China, Hefei, 230026, Anhui, China.

E-mail: yanyumse@ustc.edu.cn

[b]Max Planck Institute for Solid State Research, Heisenbergstr. 1, Stuttgart, 70569, Germany

[c]School of Materials Science and Engineering, South China University of Technology, Key Laboratory of Advanced Energy Storage Materials of Guangdong Province, Guangzhou 510641, China

# Experimental Sections

**Synthesis of monodisperse $SnO_2$ hollow nanospheres**: The template of $SnO_2$ hollow nanospheres was synthesized by a facile and low-cost hydrotheraml route. In a typical synthesis process, $K_2SnO_3 \cdot 3H_2O$ (0.768 g) and urea (0.96 g) were dissolved in a 160 mL mixture of ethanol and distilled water, which was then transferred into a Teflon-lined autoclave. The sealed vessel was then maintained at 190 °C for 15 h, and cooled naturally. The samples were collected and washed six times with ethanol and water, respectively, and dried under vacuum at 50 °C.

**Synthesis of uniform yolk-shell Sn@C nanospheres**: In a typical procedure, for carbon-coated of these $SnO_2$ hollow nanospheres, 0.34 g the as-synthesized $SnO_2$ and 1.36 g glucose were hydrothermal treated at 190 ºC for 10 h, and cooled naturally. The samples were collected and washed six times with ethanol and water, respectively, and dried under vacuum at 50 °C. Finally, these $SnO_2$@CP (carbon-rich polysaccharide) hollow nanospheres were further annealed at 700 ºC in an $H_2$/Ar flow for 6 h to obtain the precursor of yolk-shell Sn@C nanospheres.

**Synthesis of uniform yolk-shell $Sn_4P_3$@C nanospheres**: The chemical transformation of metal Sn into metal phosphide $Sn_4P_3$ was achieved by a facile and low-cost solvotheraml route. In a typical procedure, appropriate amounts (Table S1) of yolk-shell Sn@C nanospheres and red phosphorus with the molar ratio of 4:6 (Sn/P) were added into ethylenediamine solution and kept stirring for 30 min. The dispersion was transferred into a Teflon-lined autoclave. The sealed vessel was then maintained at 200 °C for 40 h, and cooled naturally. The samples were collected and washed four times with diluted HCl (0.05 mol/L), water and ethanol, respectively, and dried under vacuum at 50 °C.

**Table S1.** Summary of the selected solvotheraml reaction in ethylenediamine with the appropriate amounts of Sn@C and red phosphorus

| Group No. | Ratio Sn/P | Synthesis condition | Phase composition |
|---|---|---|---|
| 1 | 4/3 | 160 °C, 10 h | Sn + $Sn_4P_3$[a] |
| 2 | 4/3 | 200 °C, 40 h | $Sn_4P_3$ + Sn |
| 3 | 4/6 | 200 °C, 10 h | $Sn_4P_3$ + Sn |
| 4 | 4/6 | 200 °C, 40 h | $Sn_4P_3$ + Sn[a] |
| 5 | 4/6 | 200 °C, 60 h | $Sn_4P_3$ + Sn[a] |
| 6 | 4/6 | 200 °C, 40 h[b] | $Sn_4P_3$ |
| 7 | 4/9 | 200 °C, 40 h | $Sn_4P_3$ + Sn[a] + unknown phase |
| 8 | 4/15 | 200 °C, 40 h | $Sn_4P_3$ + unknown phase |

[a] Minor amount of the phase.

[b] After solvotheraml synthesis the sample was washed with diluted HCl (0.05 mol/L) for 10 h.

**Synthesis of bare $Sn_4P_3$ nano/microspheres:** Firstly, the precursor of bare Sn nanospheres was synthesized by a simple polyol method. In a typical synthesis, 0.7 g polyvinyl pyrrolidone was dissolved in 50 mL of diethylene glycol (DEG) at room temperature. The solution was heated up to 170 °C, after which 5 mmol $SnCl_2$ was added. A freshly prepared solution of $NaBH_4$ (0.872 g in 10 mL of DEG) was then added dropwise with stirring. After 20 min at 170 °C, the precursor of uniform Sn nanospheres was obtained. The chemical transformation of metal Sn nanospheres into metal phosphide $Sn_4P_3$ nano/microspheres is the same as that of yolk-shell $Sn_4P_3$@C nanospheres (see the synthesis details of yolk-shell $Sn_4P_3$@C nanospheres).

## Materials characterization

The collected products were characterized by an X-ray diffractometry (XRD) on a Rigaku-DMax 2400 diffractometer equipped with the graphite monochromatized Cu Kα radiation flux at a scanning rate of $0.02°s^{-1}$. Scanning electron microscopy (SEM) analysis was carried using a Zeiss Gemini DSM 982 scanning electron microscope. The structure of these $SnO_2$ hollow nanospheres, yolk-shell Sn@C and $Sn_4P_3$@C nanospheres was investigated by means of transmission electron microscopy (TEM, JEOL 4000FX). The amorphous carbon content in the final $Sn_4P_3$@C is about 10 wt%, as measured by weighing the residual carbon hollow nanospheres after complete etching embedded $Sn_4P_3$ nanoparticles. The tin and phosphorus contents in these yolk-shell $Sn_4P_3$@C nanospheres were measured by inductively coupled plasma atomic emission spectroscopy (ICP-AES).

## Electrochemical testing

The electrochemical performances of the as-prepared products were measured by using two-electrode Swagelok-type cells. For the preparation of the working electrode, the mixture of yolk-shell $Sn_4P_3$@C nanospheres, carbon black, and polyvinylidene fluoride (PVDF) in the weight ratio of 70:20:10 was ground in a mortar with *N*-methy1-2-pyrrolidone (NMP) as solvent to make slurry. The mass loading of the electrodes is about 1.9 mg/cm$^2$. For assembling Na-ion batteries, a Na foil was utilized as counter electrode and glass fiber (GF/D) from Whatman was used as a separator. The electrolyte was 1 M $NaClO_4$ in propylene carbonate (PC) with 5 vol% addition of fluoroethylene carbonate (FEC). CV measurements were performed on VoltaLab 80 electrochemical workstation at a scan rate of 0.1 mV $s^{-1}$. Charge/discharge (0.01–2.0 V) tests were performed on an Arbin MSTAT battery test system under ambient temperature.

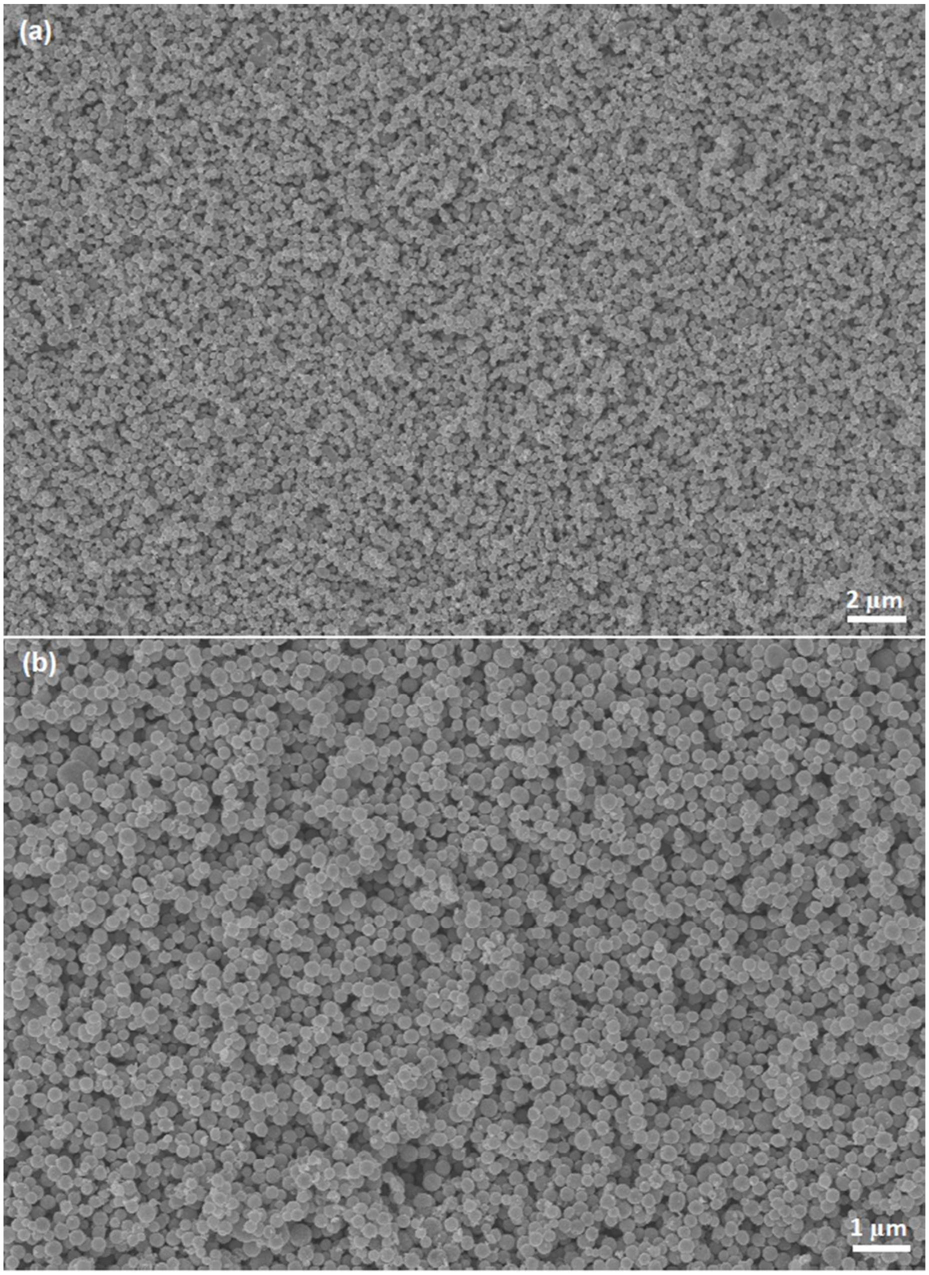

**Fig. S1** Low- and high-magnification SEM images of carbon-rich polysaccharide-coated $SnO_2$ hollow nanospheres via hydrothermally carbonization.

**Table S2** Stable specific capacities of sodium storage for yolk-shell $Sn_4P_3$@C nanospheres and only $Sn_4P_3$ yolks.

| **Current density (C)** | **Yolk-shell $Sn_4P_3$@C nanospheres (mA h $g^{-1}$)** | **Only $Sn_4P_3$ yolks (mA h $g^{-1}$)** |
|---|---|---|
| 0.1 | 711 | 790 |
| 0.2 | 648 | 720 |
| 0.4 | 586 | 651 |
| 0.8 | 523 | 581 |
| 1.5 | 455 | 505 |
| 3 | 379 | 421 |

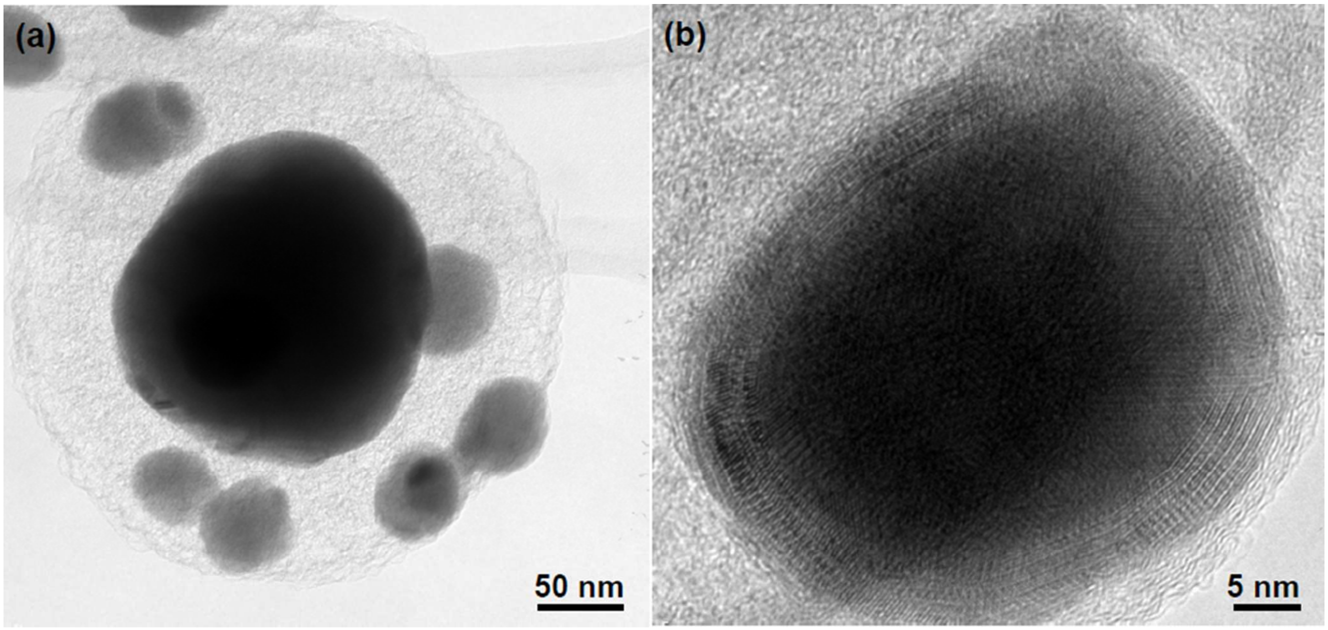

**Fig. S2** More TEM and HRTEM images of the yolk-shell Sn@C nanospheres at different selected areas, which clearly reveal their highly crystallized nature.

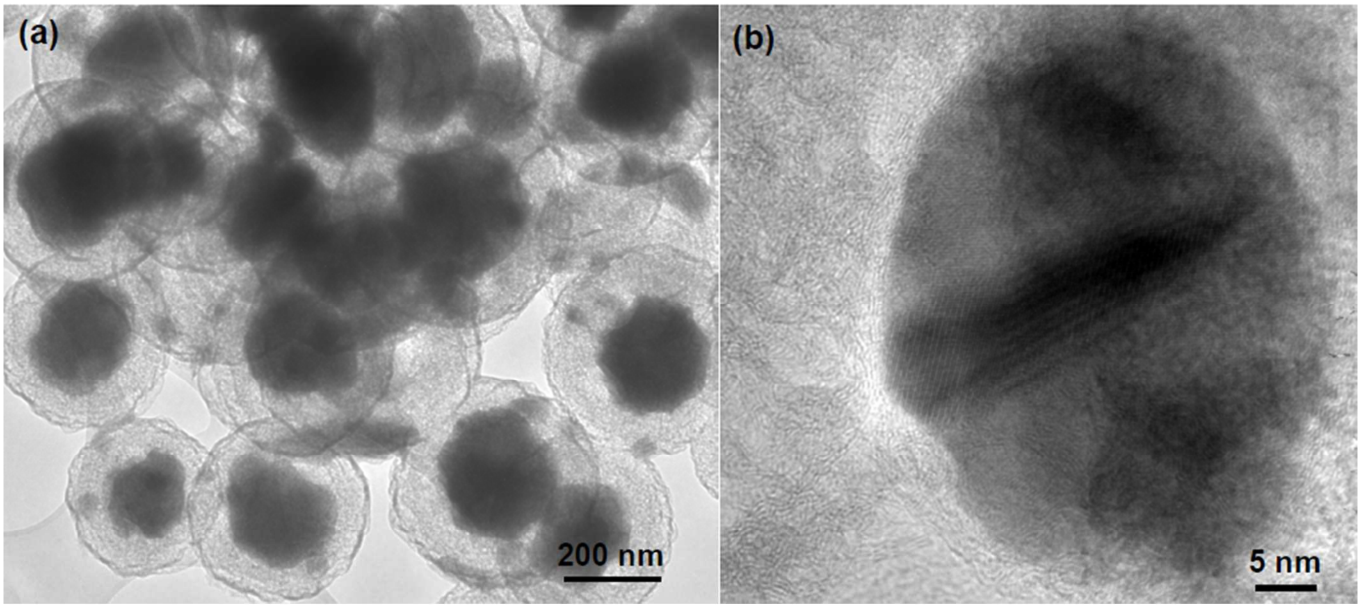

**Fig. S3** More TEM and HRTEM images of the yolk-shell $Sn_4P_3$@C nanospheres at different selected areas, which clearly reveal their highly crystallized nature.

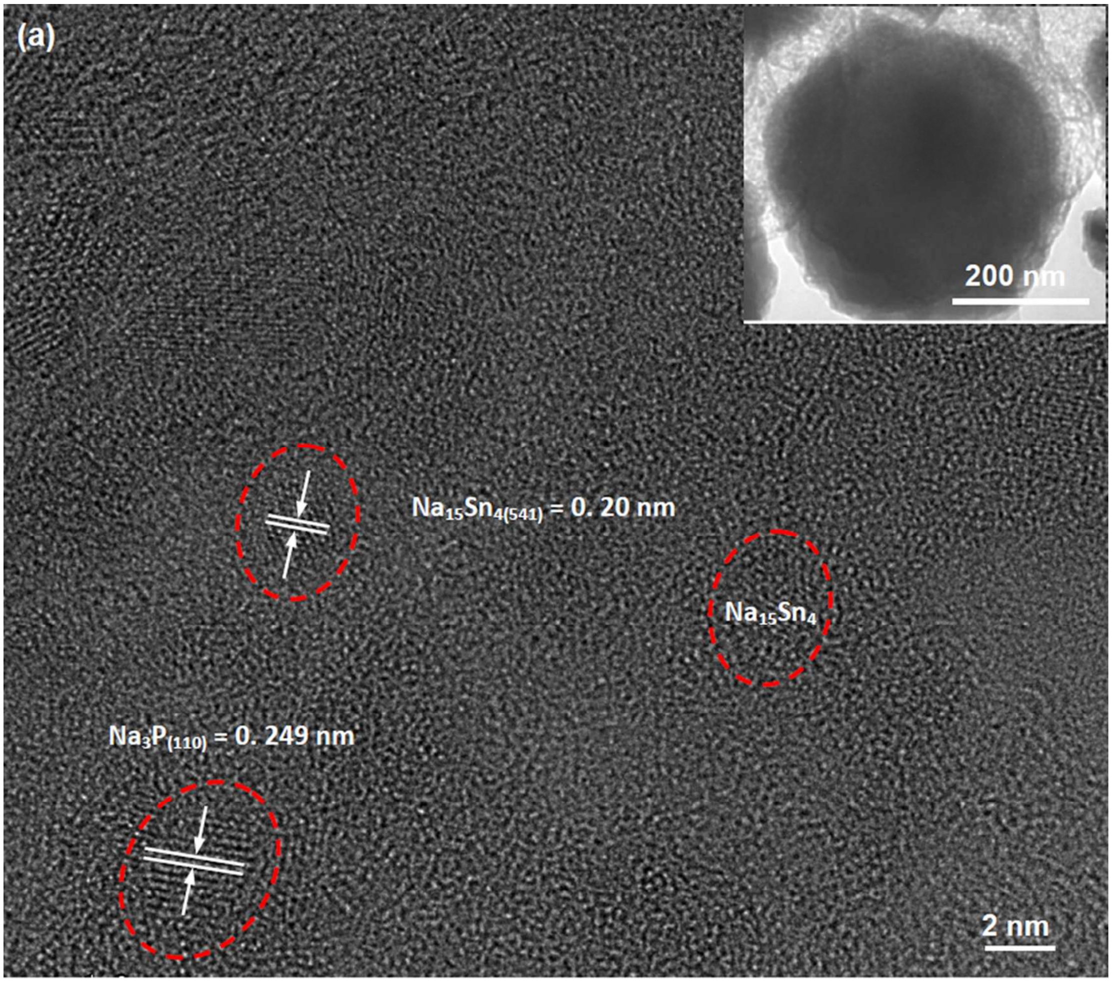

**Fig. S4** TEM and HRTEM images of yolk-shell $Sn_4P_3$@C nanospheres at the 1st discharged state, which show that the inner $Sn_4P_3$ yolk was fully expanded in the hollow carbon shell (the inset) and was converted into composites of $Na_{15}Sn_4$ and $Na_3P$.

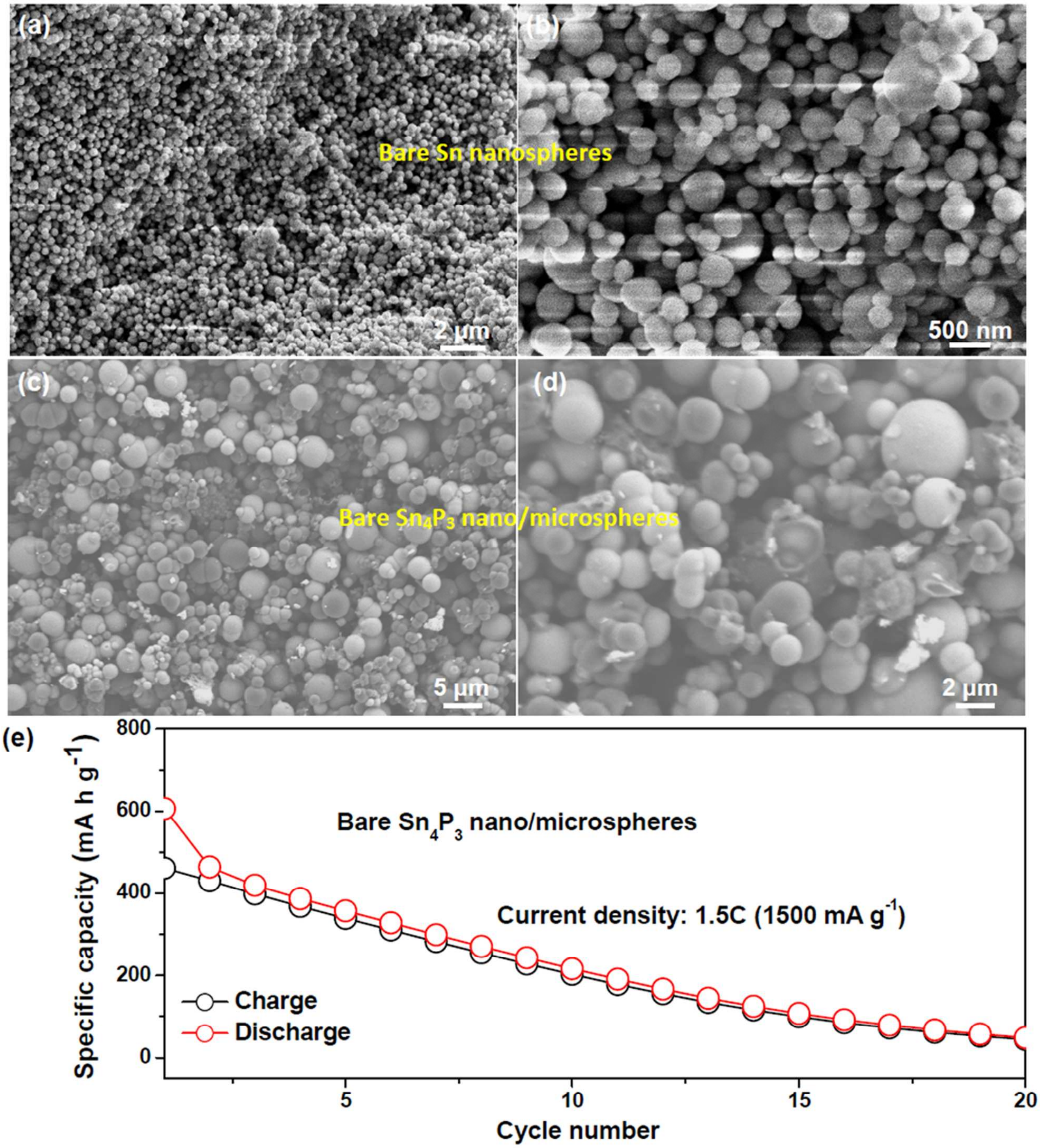

**Fig. S5** (a,b) Low- and high-magnification SEM images of the precursor of bare Sn nanospheres obtained by $NaBH_4$ reduction of $SnCl_2$; (c,d) low- and high-magnification SEM images of the product of bare $Sn_4P_3$ nano/microspheres obtained by direct phosphorization of bare Sn nanospheres (without the protection of carbon shells, the bare Sn nanospheres partly melted and aggregated together, forming much bigger microspheres); (e) Na-ion storage performance of these bare $Sn_4P_3$ nano/microspheres at 1.5C rate.

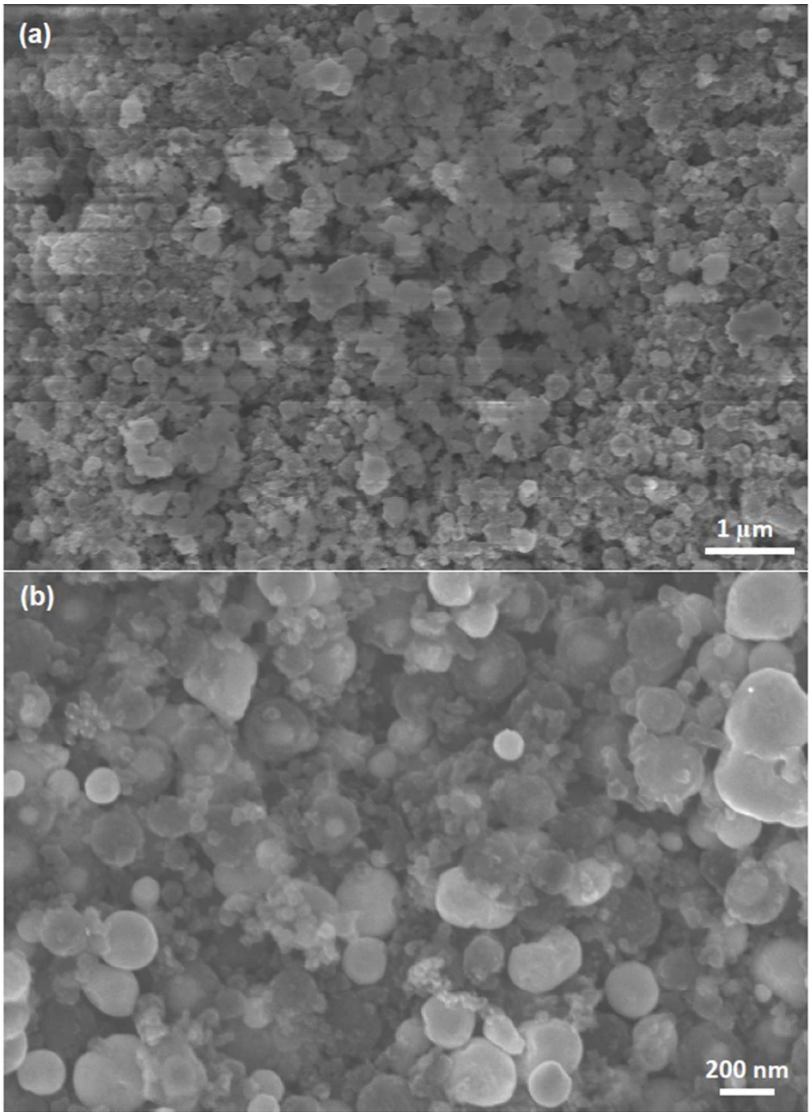

**Fig. S6** SEM images of yolk-shell $Sn_4P_3$@C nanospheres after 50 charging/discharging cycles at 0.1C rate, showing that the electroactive inner nanoparticles were still encapsulated in the carbon shells.